Björn Neubauer (Autor)

Impact of Dynamic Scatterers upon Frequency- and Amplitude-Modulation

A Theoretical and Practical Treatise in the Context of the Doppler-VOR and Wind Turbines

https://cuvillier.de/de/shop/publications/8525

1. Prologue

The way, in which this thesis is organized, is given in the summary both in writing as well as in a graphical manner; see page 211ff.

1.1. Summing Two Oscillations of Equal Angular Velocity

A major backbone of the theory presented in the work at hand consists of summing one intended and one unintended oscillation, in order to investigate to which extent the resulting oscillation differs from the intended one. Prior to embedding this task in a technical context, it is treated purely mathematical. An oscillation can be described via the angular functions cosine or sine

$$\tilde{U}_{\Re}(t) = U\cos[\omega_u t - \phi_u] \tag{1.1}$$
$$\tilde{U}_{\Im}(t) = U\sin[\omega_u t - \phi_u], \tag{1.2}$$

with U as amplitude, ω_u as angular velocity and ϕ_u as instantaneous phase. Additionally, a single oscillation can be thought of as vector $\vec{U}(t)$ in the complex plane, being attached at its base to the coordinate system's origin around which it spins counterclockwise for growing t with the angular velocity ω_u. Then $\tilde{U}_{\Re}(t)$ describes the real part, that is to say the projection of the vector $\vec{U}(t)$ onto the real axis and $\tilde{U}_{\Im}(t)$ the projection onto the imaginary axis corresponding to the imaginary part. Figure 1.1 visualizes this context, whereas 1.1a depicts both the vector $\vec{U}(t)$ and its projections onto the real and imaginary axis for an arbitrary time t, respectively, and 1.1b shows its projection onto the real axis versus time t.

The expression capturing this relation of a vector's/complex number's representation by its phase and absolute value on the one hand and on the other hand by its real and imaginary part is Euler's relation, which applied on $\vec{U}(t)$ is:

$$Ue^{j[\omega_u t - \phi_u]} = U(\cos[\omega_u t - \phi_u] + j\sin[\omega_u t - \phi_u]) \tag{1.3}$$

To summate two vectors, $\vec{U}(t)$ and $\vec{A}(t)$, here, both of identical angular velocity ω_u, but different in phase and with $A < U$, the base of one vector is attached to the tip of the other, as shown in figure 1.2. The resulting vector $\vec{R}(t)$ corresponds to the straight line between the base of the first one and the tip of the second one. Choosing time t to equal the ratio ϕ_u/ω_u corresponds to pivoting both $\vec{U}(t)$ and $\vec{A}(t)$ and thus the resulting $\vec{R}(t)$ around the origin of the gray indicated coordinate system so that $\vec{U}$ lays on the positive abscissa. Figure 1.3 depicts this constellation in which the base of $\vec{A}(t)$ is attached to the tip of $\vec{U}(t)$ with the angle $\phi_u - \phi_a$ relative to the abscissa. This angle follows directly from the argument of $\vec{A}(t)$ for $t = \phi_u/\omega_u$. There are two ways of calculating the length of $\vec{R}$: One is by applying the law of cosines. The angle between $\vec{U}(t)$ and $\vec{A}(t)$ is calculated to $\pi - \alpha$ as illustrated in figure 1.3:

$$R = \sqrt{U^2 + A^2 - 2UA\cos[\pi - (\phi_u - \phi_a)]} \tag{1.4}$$
$$= \sqrt{U^2 + A^2 + 2UA\cos[\phi_u - \phi_a]} \tag{1.5}$$

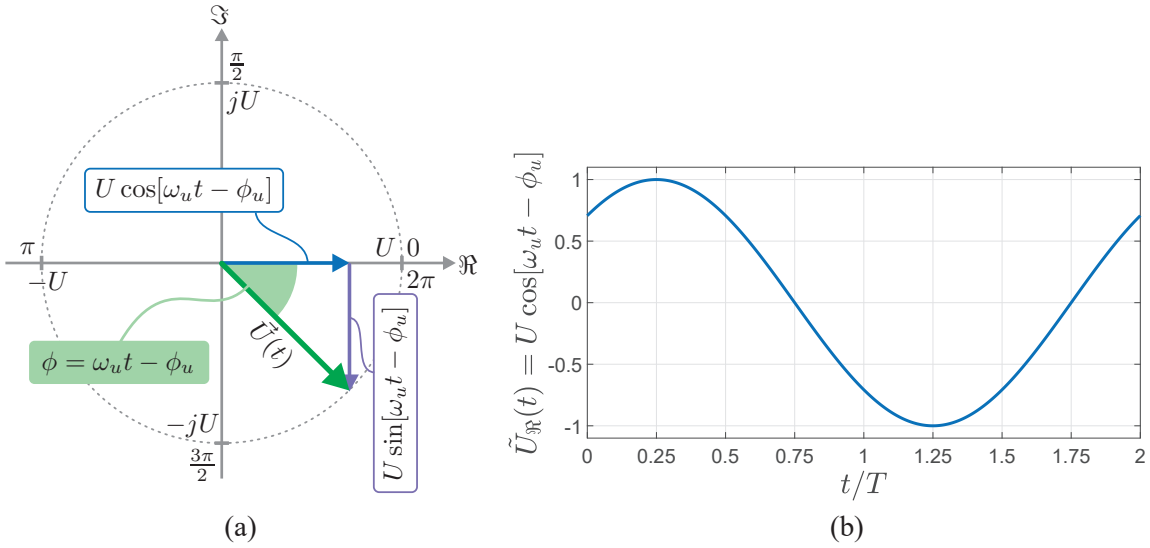

Figure 1.1.: (a) $\vec{U}(t)$ in the complex plane and its projections onto $\Re$ and $\Im$, (b) $\tilde{U}_{\Re}(t)$ versus time t.

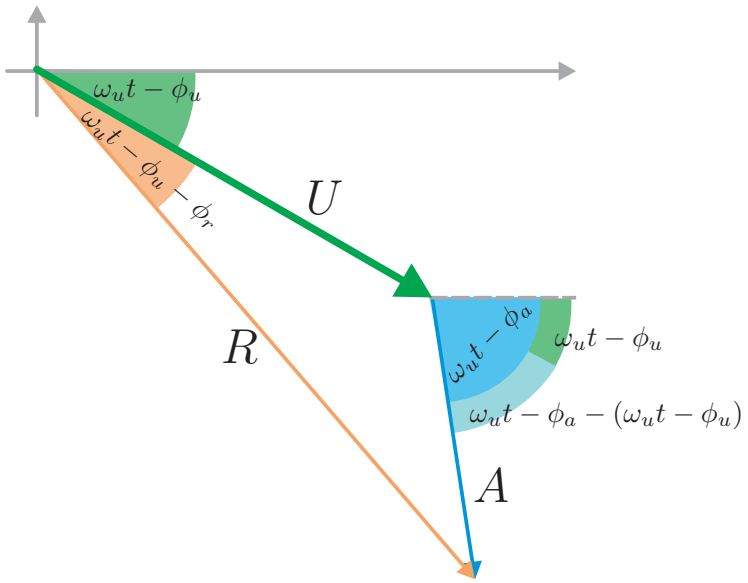

Figure 1.2.: $\vec{U}(t) + \vec{A}(t) = \vec{R}(t)$.

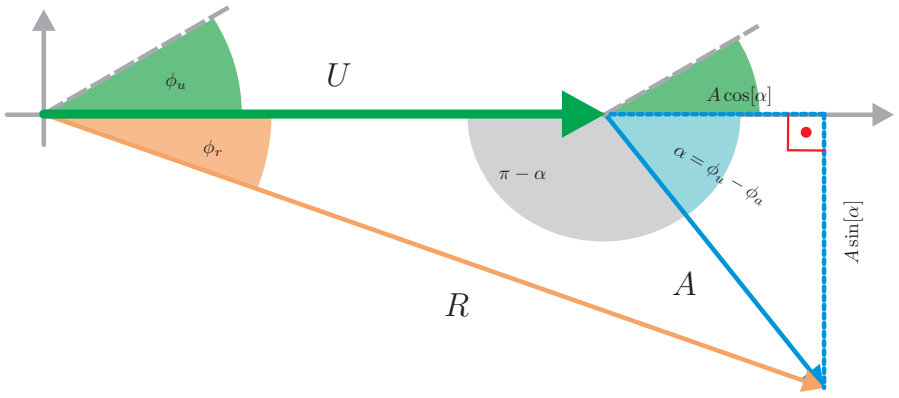

Figure 1.3.: $\vec{U}(t) + \vec{A}(t) = \vec{R}(t)$ for $t = \frac{\phi_u}{\omega_u}$.

The second option consists of applying the Pythagorean theorem:

$$R = \sqrt{(U + A\cos[\phi_u - \phi_a])^2 + (A\sin[\phi_u - \phi_a])^2} \tag{1.6}$$

$$= \sqrt{U^2 + 2UA\cos[\phi_u - \phi_a] + \underbrace{A^2\cos^2[\phi_u - \phi_a] + A^2\sin^2[\phi_u - \phi_a]}_{=A^2}} \tag{1.7}$$

$$= \sqrt{U^2 + A^2 + 2UA\cos[\phi_u - \phi_a]}. \tag{1.8}$$

Also depicted in figure 1.3 the phase angle ϕ_r of the resulting vector is given by the inverse tangent of the imaginary part of $\vec{R}(\phi_u/\omega_u)$, which constitutes the opposite leg, divided by the real part of $\vec{R}(\phi_u/\omega_u)$, which resembles the adjacent leg:

$$\phi_r = \arctan\left[\frac{A\sin[\phi_u - \phi_a]}{U + A\cos[\phi_u - \phi_a]}\right]. \tag{1.9}$$

After these preparing considerations, the initial intention to express two oscillations by a single one is presumed. To start with both summands, $\tilde{U}(t)$, $\tilde{A}(t)$, are expressed as real part of a complex number, each given by its absolute value and phase. Then $e^{j[\omega_u t - \phi_u]}$ is factored out, which corresponds to the above mentioned pivoting, so that $\vec{U}(t)$ lays on the positive abscissa; (1.12). $R \cdot e^{j\phi_r}$ describes the resulting vector as previously discussed, before $e^{j(\omega_u t - \phi_u)}$ is factored in again; (1.14). Next the operator $\Re$ reduces the complex number to its real part, before the expressions (1.8), (1.9) are inserted.

$$U\cos[\omega_u t - \phi_u] + A\cos[\omega_u t - \phi_a] \tag{1.10}$$

$$\overset{(A.1)}{=} \Re\left\{ Ue^{j[\omega_u t - \phi_u]} + Ae^{j[\omega_u t - \phi_a \overbrace{-\phi_u + \phi_u}^{=+0}]} \right\} \tag{1.11}$$

$$= \Re\left\{ e^{j[\omega_u t - \phi_u]} \left(\underbrace{U + Ae^{j[\phi_u - \phi_a]}}_{\text{see fig. 1.3}} \right) \right\} \tag{1.12}$$

$$= \Re\left\{ e^{j[\omega_u t - \phi_u]} R \cdot e^{j\phi_r} \right\} \tag{1.13}$$

$$= \Re\left\{ R \cdot e^{j[\omega_u t - \phi_u + \phi_r]} \right\} \tag{1.14}$$

$$= R\cos[\omega_u t - \phi_u + \phi_r] \tag{1.15}$$

$$\overset{(1.8)}{\overset{(1.9)}{=}} \sqrt{U^2 + A^2 + 2UA\cos[\phi_u - \phi_a]} \cdot \cos\left[\omega_u t - \phi_u + \underbrace{\arctan\left[\frac{A\sin[\phi_u - \phi_a]}{U + A\cos[\phi_u - \phi_a]}\right]}_{=:\phi_r}\right]. \tag{1.16}$$

$$\overset{\alpha:=\phi_u-\phi_a}{\Longrightarrow} \phi_r(\alpha) = \arctan\left[\frac{A\sin[\alpha]}{U + A\cos[\alpha]}\right] \tag{1.17}$$

The expression (1.16) describes the resulting time signal. Due to adding the oscillation $\tilde{A}(t)$ to the oscillation $\tilde{U}(t)$, both of the identical angular velocity ω_u, R's amplitude as well as its phase ϕ_r do change depending on U, A, α. ϕ_r describes the extent to which the resulting oscillation's phase deviates from $\tilde{U}(t)$'s phase. Both of the following two figures, 1.4 and 1.5, visualize $\phi_r(\alpha)$ for several ratios $\frac{A}{U}$ with $U = 1$. The angles are given in degree. For low

ratios of $\frac{A}{U}$ the sinus clearly dominates the course, due to the fact that the argument of the inverse tangents approximates the inverse tangents well as long as the argument remains footnotesize of value. Nevertheless, even by eye-inspection it can be observed, that the maximal phase deviation rapidly grows and moves from $\alpha = 90°$ to $\alpha = 180°$ for an increasing ratio $\frac{A}{U}$. When $\frac{A}{U}$ reaches unity, $\phi_r(\alpha)$ resembles a saw tooth and for growing α it experiences a phase jump from $+90°$ to $-90°$ at $\alpha = 180°$. Due to $\arctan$, $\sin$ resembling an odd function, that is $-f(x) = f(-x)$, and the $\sin$, $\cos$ being of the same periodicity, $\phi_r(\alpha)$ constitutes an odd, periodic function. Additionally, in figure 1.6 the length R of the resulting vector is plotted versus the phase difference $\alpha := \phi_u - \phi_a$. The plotted domain is chosen such, that it allows to clearly recognize the different curvatures of the extrema by comparing minima and maxima.

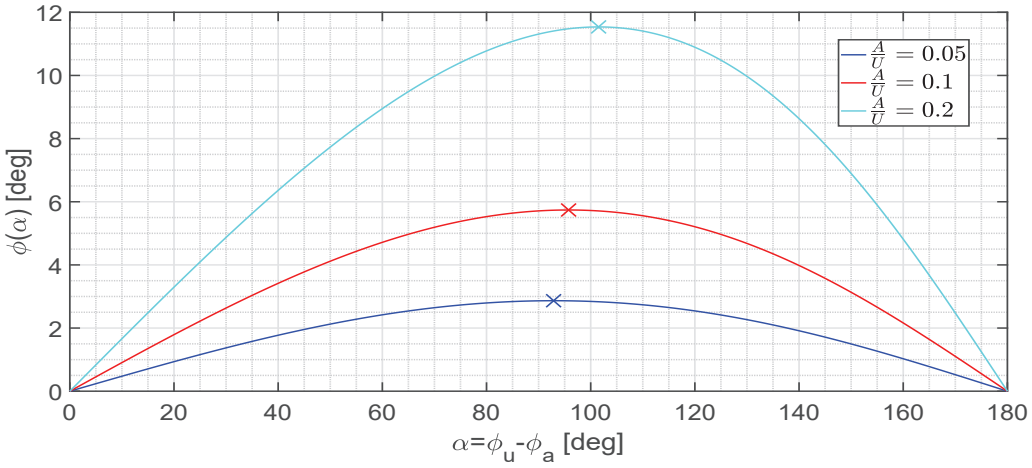

Figure 1.4.: Phase deviation $\phi_r(\alpha)$ of $\tilde{R}(t)$ with respect to $\tilde{U}(t)$ due to $\tilde{U}(t) + \tilde{A}(t)$ versus $\alpha = \phi_a - \phi_u$ for $\frac{A}{U} = 0.05, 0.1, 0.2$. Maxima at $(\alpha_{max}, \phi_{max}) = (92.89, 2.87)$, $(95.76, 5.74)$, $(101.55, 11.54)$, all in degree.

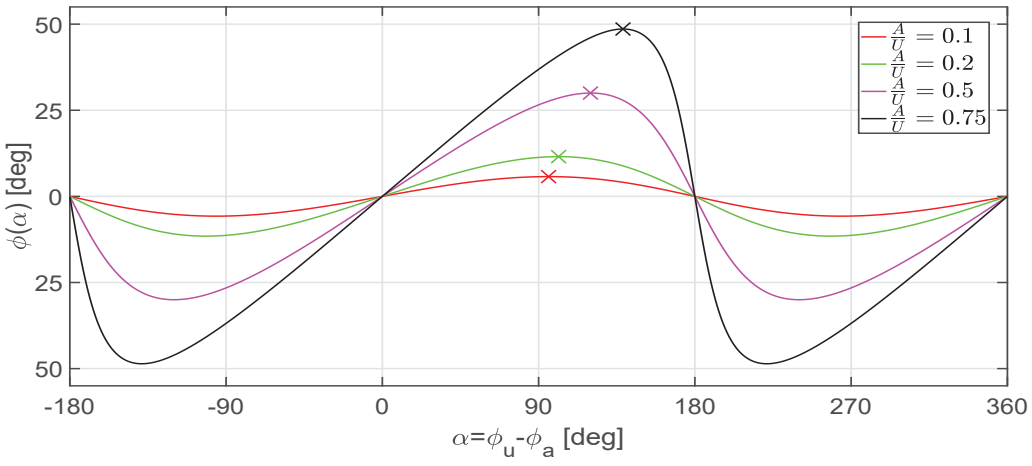

Figure 1.5.: $\phi_r(\alpha)$ for $\frac{A}{U} = 0.1, 0.2, 0.5, 0.75$ with $(\alpha_{max}, \phi_{max}) = (95.764, 5.7)$, $(101.52, 11.54)$, $(11.88, 30)$, $(138.6, 48.59)$, all in degree.

In the context of the thesis at hand, the value of this phase deviation, its maximum in particular, is of major interest. This interest can be addressed by solving the extreme-value problem based

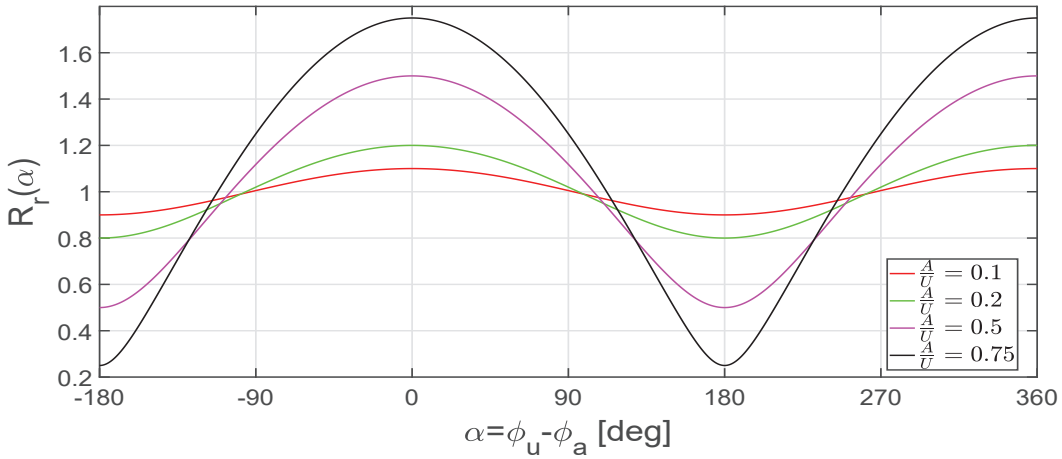

Figure 1.6.: $R(\alpha)$ for $\frac{A}{U} = 0.1, 0.2, 0.5, 0.75$.

on the derived, analytical expression (1.17). To solve an extreme-value problem, the first and the second derivation with respect to the variable of interest are required. Here, the variable of interest is given by $\alpha := \phi_u - \phi_a$. The first derivation calculates to

$$\frac{d\phi_r(\alpha)}{d\alpha} = \frac{d}{d\alpha}\arctan\left[\frac{A\sin[\alpha]}{U + A\cos[\alpha]}\right] \tag{1.18}$$

$$= \frac{1}{1+\left(\frac{A\sin[\alpha]}{U+A\cos[\alpha]}\right)^2}\cdot\frac{A\cos[\alpha](U+A\cos[\alpha]) - A\sin[\alpha](-A\sin[\alpha])}{(U+A\cos[\alpha])^2} \tag{1.19}$$

$$= \frac{UA\cos[\alpha] + \overbrace{A^2\cos^2[\alpha]+\sin^2[\alpha]}^{=A^2}}{(U+A\cos[\alpha])^2 + A^2\sin^2[\alpha]} \tag{1.20}$$

$$= \frac{UA\cos[\alpha] + A^2}{U^2 + 2UA\cos[\alpha] + A^2\cos^2[\alpha] + A^2\sin^2[\alpha]} \tag{1.21}$$

$$= A\frac{U\cos[\alpha] + A}{U^2 + 2UA\cos[\alpha] + A^2}, \tag{1.22}$$

and the seccond to

$$\frac{d^2\phi_r(\alpha)}{d\alpha^2}$$

$$= A\frac{-U\sin[\alpha]\left(U^2 + 2UA\cos[\alpha] + A^2\right) - (U\cos[\alpha] + A)(-2UA\sin[\alpha])}{(U^2 + 2UA\cos[\alpha] + A^2)^2} \tag{1.23}$$

$$= A\frac{-U^3\sin[\alpha] - 2U^2A\sin[\alpha]\cos[\alpha] - UA^2\sin[\alpha] + 2U^2A\sin[\alpha]\cos[\alpha] + 2UA^2\sin[\alpha]}{(U^2 + 2UA\cos[\alpha] + A^2)^2} \tag{1.24}$$

$$= A\frac{-U^3\sin[\alpha] + UA^2\sin[\alpha]}{(U^2 + 2UA\cos[\alpha] + A^2)^2} \tag{1.25}$$

$$= AU\frac{(A^2 - U^2)\sin[\alpha]}{(U^2 + 2UA\cos[\alpha] + A^2)^2}. \tag{1.26}$$

For an extremum the first derivation equals zero for $\alpha = \alpha_{ex}$. Thus, (1.22) is set equal to zero and solved for α_{ex}:

$$\frac{d\phi_r(\alpha_{ex})}{d\alpha} \stackrel{!}{=} 0 \Longrightarrow U\cos[\alpha_{ex}] + A = 0 \tag{1.27}$$

$$\cos[\alpha_{ex}] = -\frac{A}{U} \tag{1.28}$$

$$\alpha_{ex} = \arccos[-\frac{A}{U}]. \tag{1.29}$$

In order to determine, whether this extreme is a mini- or maximum, α_{ex} is inserted into (1.26). An outcome below zero identifies the extremum at hand as a local maximum. As the denominator is to the power of two, it will not change the sign of the ratio. Thus, only the nominator remains to be investigated:

$$AU(A^2 - U^2)\sin[\arccos[-\frac{A}{U}]] \tag{1.30}$$

$$\stackrel{(A.8)}{=} AU \cdot (A^2 - U^2) \cdot \sqrt{1 - (-\frac{A}{U})^2}. \tag{1.31}$$

Both the first and third factor are greater than zero, whereas the second one is footnotesizeer than zero, due to $A < U$. In case of $A > U$ both would reverse their roles with one another. Thus, the second derivation of the phase deviation ϕ_r with respect to the phase difference α is footnotesizeer than zero at α_{ex}, which in turn proves the extremum in the interval $\alpha \in [0, \pi]$ to be a maximum; $\alpha_{ex} =: \alpha_{max}$.
Inserting this α_{max} into (1.9) determines the value of the maximal phase deviation.

$$\phi_r(\alpha_{max}) = \arctan\left[\frac{A\sin\left[\arccos[-\frac{A}{U}]\right]}{U + A\cos\left[\arccos[-\frac{A}{U}]\right]}\right] \tag{1.32}$$

$$\stackrel{(A.8)}{=} \arctan\left[\frac{A\sqrt{1 - (-\frac{A}{U})^2}}{U + A(-\frac{A}{U})}\right] \tag{1.33}$$

$$= \arctan\left[\frac{\frac{A}{U}\sqrt{U^2 - A^2}}{\frac{U^2 - A^2}{U}}\right] \tag{1.34}$$

$$= \arctan\left[\frac{A\sqrt{U^2 - A^2}}{\sqrt{U^2 - A^2}\sqrt{U^2 - A^2}}\right] \tag{1.35}$$

$$= \arctan\left[\frac{A}{\sqrt{U^2 - A^2}}\right] \tag{1.36}$$

$$= \arctan\left[\frac{1}{\sqrt{\frac{1}{(\frac{A}{U})^2} - 1}}\right] \tag{1.37}$$

Before plotting $\phi_r(\alpha_{max})$ a more descriptive treatment of the mechanism at work proceeds in order to offer a better intuitive understanding. Figure 1.7 depicts vector $\vec{U}$ in green, the added vector $\vec{A}$ in blue at two different angles α as well as the resulting vector $\vec{R} = \vec{U} + \vec{A}$ in orange including its phase ϕ_r relative to $\vec{U}$. Additionally, the blue, dotted circle indicates all possible positions which the tip of $\vec{A}$ can take by $\vec{A}$ orbiting at its base around the tip of $\vec{U}$. Thus, this orbit and the base of $\vec{U}$ illustrate all possible resulting vectors $\vec{R}$. Starting with $\alpha = 0$, the resulting phase deviation ϕ_r equals zero whilst the absolute value possesses it maximal value $R_{max} = U + A\cos[0] = U + A$. By increasing α, the tip of $\vec{A}$ moves counterclockwise (ccw) along the orbit, thus increasing the relative phase ϕ_r between $\vec{U}$ and $\vec{R}$. Simultaneously, the absolute value R shrinks. R continuous to shrink till it passes its minimal value $R_{min} = U + A\cos[\pi] =$

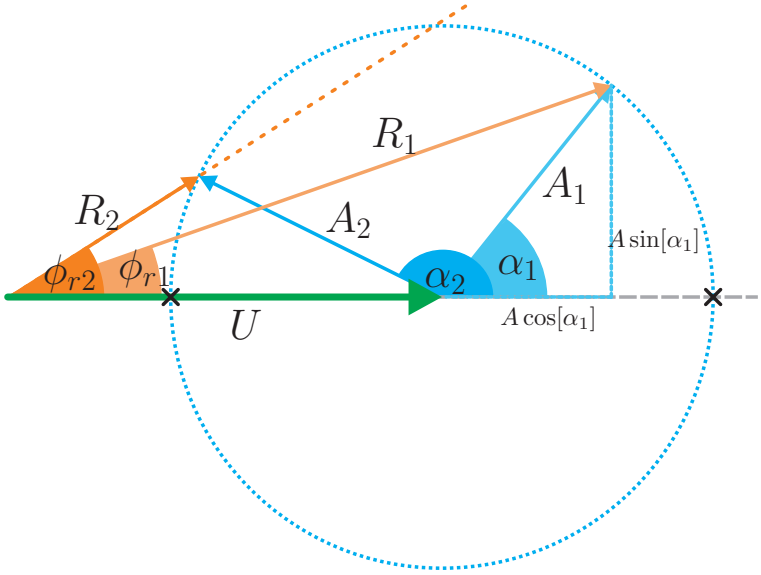

Figure 1.7.: Vector addition of $\vec{U}$, $\vec{A}$.

$U - A$ and increases again till the initial situation is reached at $\alpha = 2\pi$. Thus, the initially increasing ϕ_r reaches a maximum value at an α_{max} before decreasing, passing zero and due to the symmetry with respect to the abscissa passes through a minimum at $\alpha_{min} = 2\pi - \alpha_{max}$ with $\phi_{r,min} = -\phi_{r,max}$ before equaling zero again at $\alpha = 2\pi$. During the course of the previously described movement, $\vec{R}$, its tip always ending on the blue orbit, "cuts" this orbit, see figure 1.7, before its tip passes through the point with $\phi(\alpha_{max})$ in which it is directed outermost away from $\vec{U}$'s tip, see figure 1.8. For α_{max} the vector $\vec{R}$ lays on the tangent through the base of $\vec{U}$ and the blue orbit and thus in turn has to be perpendicular to $\vec{A}$ as the latter resembles the radius of the mentioned orbit. As $\vec{U}$,$\vec{A}$,$\vec{R}$ constitute a rectangular triangle for $\phi(\alpha_{max})$ with U as hypotenuse a (half-)circle can be drawn (above)around U being its diameter. Then, wherever depending on A, "Thales" (half-)circle and the blue orbit intersect, $\vec{R}$ has taken on its maximal phase deviation for $\alpha_{max} \in [\frac{\pi}{2}, \pi[$ and its minimal phase deviation for $\alpha_{min} \in]\pi, \frac{3}{2}\pi]$, respectively.

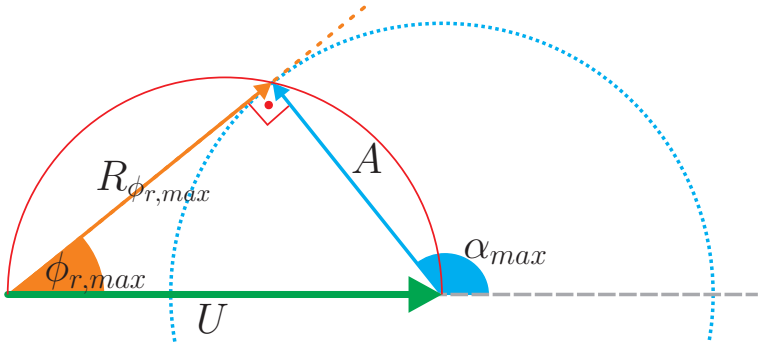

Figure 1.8.: Resulting vector with maximal phase deviation $\phi(\alpha_{max})$.

In addition to deriving the expression (1.36) for $\phi_r(\alpha_{max})$ by solving an extreme-value-problem, the knowledge of $\vec{U}$,$\vec{A}$,$\vec{R}$ forming a rectangular triangle can be put to use in order to derive a different expression for $\phi_r(\alpha_{max})$ as done in by Geise and Geise in [8]: U resembles the hypotenuse and A the opposite leg. Thus,

$$\phi_r(\alpha_{max}) \quad = \quad \arcsin[\frac{A}{U}] \tag{1.38}$$

describes the desired angle. Figure 1.9 serves to gain the insight that both given expressions, (1.36),(1.38), for $\phi_r(\alpha_{max})$ equal one another. Geise and Geise deduce (1.38) from the triangle (a), (r), (u). Whilst (1.9) has been derived relaying on a scatch of the situation with $\alpha \in [0, \frac{\pi}{2}[$, see figure 1.3 in order to ease the understanding. Nevertheless it holds true for values of α beyond $\frac{\pi}{2}$, because the cosine of $\alpha \in [\frac{\pi}{2}, \frac{3}{2}\pi]$ yields a negative value. Thus, $U + A\cos[\alpha_{max}]$ describes the adjacent and $A\sin[\alpha_{max}]$ the opposite leg of the triangle (a), (ar), (u). Figure 1.10 depicts the phase deviation α_{max} between $\vec{A}$, $\vec{U}$ in degree versus the ratio $\frac{A}{U}$,

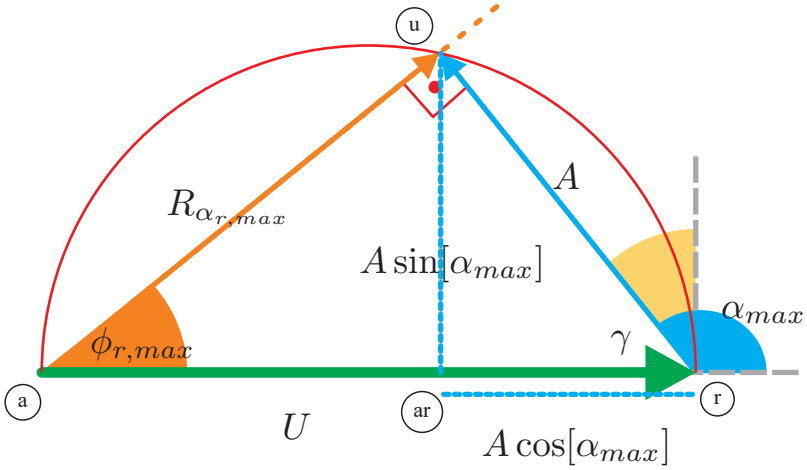

Figure 1.9.: Graph displaying the orbits of the vectors $\vec{U}$, $\vec{A}$, $\vec{R}$.

which relates to the maximal phase deviation ϕ_{max}, between $\vec{U}$ and the resulting $\vec{R}$. Inserting this α_{max} into (1.17) yields the dependency as figure 1.11 visualizes it. The graph, $\phi(\alpha_{max})$ versus α_{max} resembles a straight line. This can be easily understood by envision that the triangle involved is a rectangular one: Thus, $\gamma = \frac{\pi}{2} - \phi_{r,max}$ by which α can be described as $\pi - \gamma$. Inserting the expression for γ and solving for the phase deviation of interest yields the equation of a line: $\phi_{r,max} = \alpha_{max} - \frac{\pi}{2}$, with the y-intercept at $-\frac{\pi}{2}$. Hence, the maximal phase deviation between $\vec{U}$,$\vec{R}$ is a quarter period lower than the related phase deviation α_{max} between $\vec{U}$, $\vec{A}$.

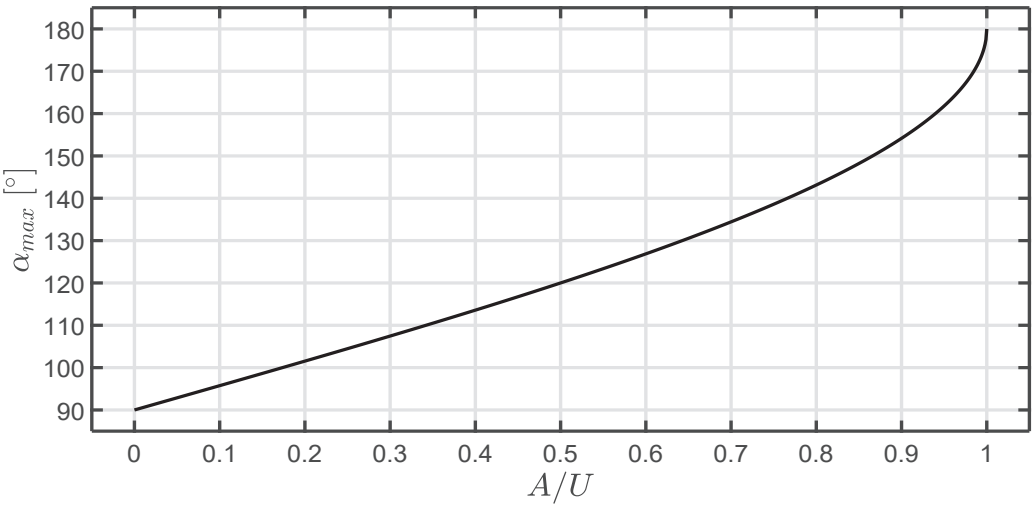

Figure 1.10.: α_{max} between $\vec{U}$, $\vec{A}$ versus $\frac{A}{U}$ for $U = 1$ causing $\phi_{r,max}$.

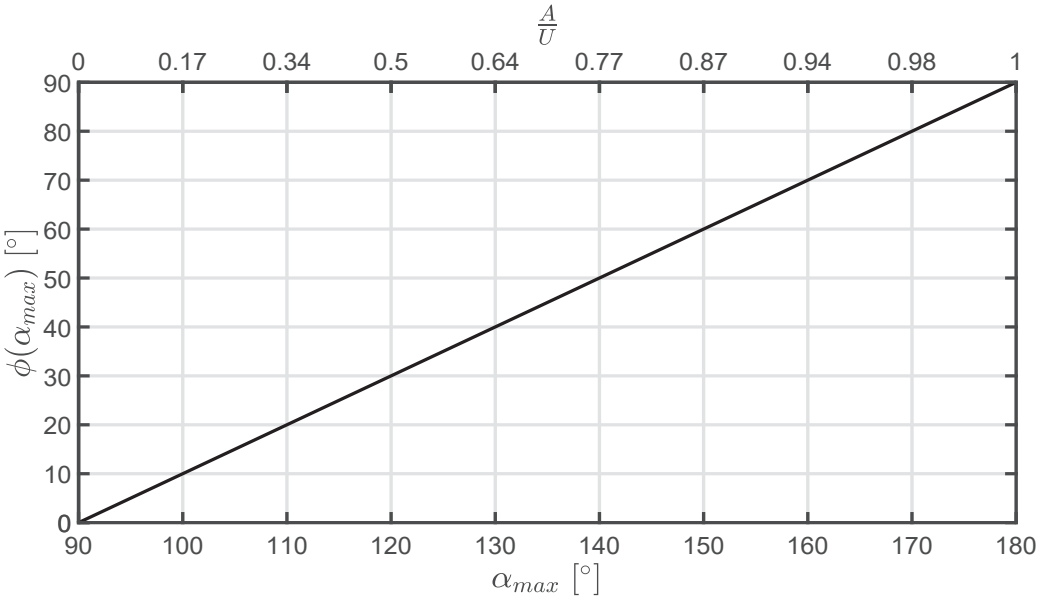

Figure 1.11.: $\phi_{r,max}$ versus $\alpha_{r,max}$. Both in degree.

Figure 1.12 illustrates the dependency of $\phi_{r,max}$ in degree directly plotted versus the ratio $\frac{A}{U}$. The fact that the plots of both (1.36) in yellow and (1.38) in dashed black perfectly match, illustrates once more that these two expressions are equivalent. In order to allow for a better comparison, the figures 1.11, 1.12 do have a second x-axis at the top of the frame, labeled with the values corresponding to the x-axis at the bottom.

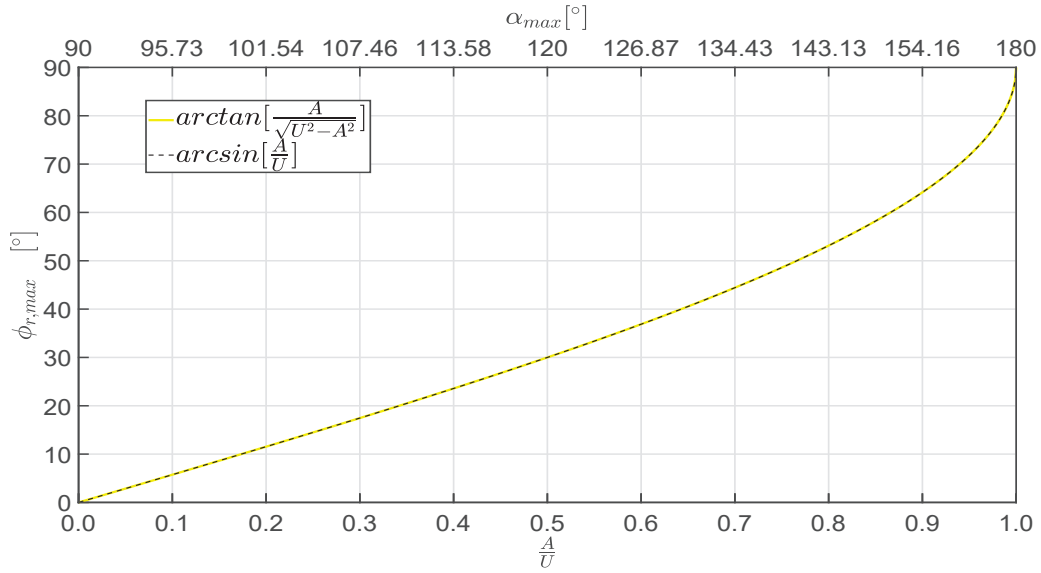

Figure 1.12.: $\phi_{r,max}$ versus $\frac{A}{U}$ for $U = 1$.

1.2. Summing Two Oscillations of Different Angular Velocity

In the previous section, the sum of two oscillations, different in phase but of the same angular velocity, is expressed as a single oscillation. In compliance with the Fourier analysis, this resulting oscillation possesses the same angular velocity as its components. Further its phase, which in the work at hand comprises the major interest, is investigated with respect to its course

and its extrem/peak values depending on the involved parameters; A, U. On this basis, the sum of two oscillations of different phase and now as well of different angular velocity is expressed as a single oscillation:

$$U\cos[\omega_u t-\phi_u]+A\cos[\omega_a t-\phi_a] \tag{1.39}$$

$$\overset{(A.1)}{=} \Re\left\{Ue^{j[\omega_u t-\phi_u]}+Ae^{j[\omega_a t-\phi_a}\overbrace{+\omega_u t-\phi_u-\omega_u t+\phi_u]}^{=+0}\right\} \tag{1.40}$$

$$= \Re\left\{e^{j[\omega_u t-\phi_u]}\left(U+Ae^{j[(\omega_a-\omega_u)t+\phi_u-\phi_a]}\right)\right\} \tag{1.41}$$

$$= \Re\left\{e^{j[\omega_u t-\phi_u]}R_t\cdot e^{j\phi_{rt}}\right\} \tag{1.42}$$

$$= \Re\left\{R_t\cdot e^{j[\omega_u t-\phi_u+\phi_{rt}]}\right\} \tag{1.43}$$

$$= R_t\cos[\omega_u t-\phi_u+\phi_{rt}] \tag{1.44}$$

$$\overset{(1.8)}{\overset{(1.9)}{=}} \sqrt{U^2+A^2+2UA\cos[(\omega_a-\omega_u)t+\phi_u-\phi_a]} \cdot\cos\left[\omega_u t-\phi_u+\underbrace{\arctan\left[\frac{A\sin[(\omega_a-\omega_u)t+\phi_u-\phi_a]}{U+A\cos[(\omega_a-\omega_u)t+\phi_u-\phi_a]}\right]}_{=:\phi_{rt}}\right]. \tag{1.45}$$

With $\Delta\omega := \omega_a-\omega_u$ and $\alpha=\phi_u-\phi_a$ the absolute value R_t and the phase ϕ_{rt} can be written as:

$$R_t(t) = \sqrt{U^2+A^2+2UA\cos[\Delta\omega t+\alpha]} \tag{1.46}$$

$$\phi_{rt}(t) = \arctan\left[\frac{A\sin[\Delta\omega t+\alpha]}{U+A\cos[\Delta\omega t+\alpha]}\right]. \tag{1.47}$$

Besides the "angular velocity" $\Delta\omega$ times t in the angular functions (1.8), (1.32) are identical to (1.46), (1.47).
Factoring out $\Delta\omega$ from ϕ_{rt}'s argument offers directly the insight, that the course is shifted to lower values of t by $\frac{\alpha}{\Delta\omega}$ for $\alpha,\Delta\omega>0$. The periodicity can be derived from the involved angular velocities:

$$\Delta\omega=\omega_a-\omega_u=2\pi(f_a-f_u)=\frac{2\pi}{\Delta T} \tag{1.48}$$

$$\overset{\text{equating coef.}}{\Longrightarrow} \Delta T=\frac{1}{f_a-f_u}=\frac{1}{\frac{1}{T_a}-\frac{1}{T_u}}=\frac{T_aT_u}{T_u-T_a}. \tag{1.49}$$

Figure 1.13 depicts the course of the resulting phase deviation ϕ_{rt} in degree versus time t in seconds calculated for $f_u=30$ Hz, $f_a=35$ Hz and $\alpha=\frac{\pi}{3}$ in an exemplary manner.
Due to the similarities of the situations ϕ_r and ϕ_{rt} are described by the same function. Therefore, the values of the extrema are identical aside from occurring related to different variables. They occur when the argument takes on the values determined in subsection 1.1. Instead of solving the extreme-value problem again, the argument of ϕ_{rt} can be set equal to α_{max} of ϕ_r, (1.17), and solved for the variable $t=t_{max}$:

$$\Delta\omega t_{max}+\alpha \overset{!}{=} \alpha_{max} \tag{1.50}$$

$$\Longleftrightarrow \Delta\omega t_{max}+\alpha = \arccos[-\frac{A}{U}] \tag{1.51}$$

$$\Longleftrightarrow t_{max} = \frac{1}{\Delta\omega}\big(\arccos[-\frac{A}{U}-\alpha]\big). \tag{1.52}$$

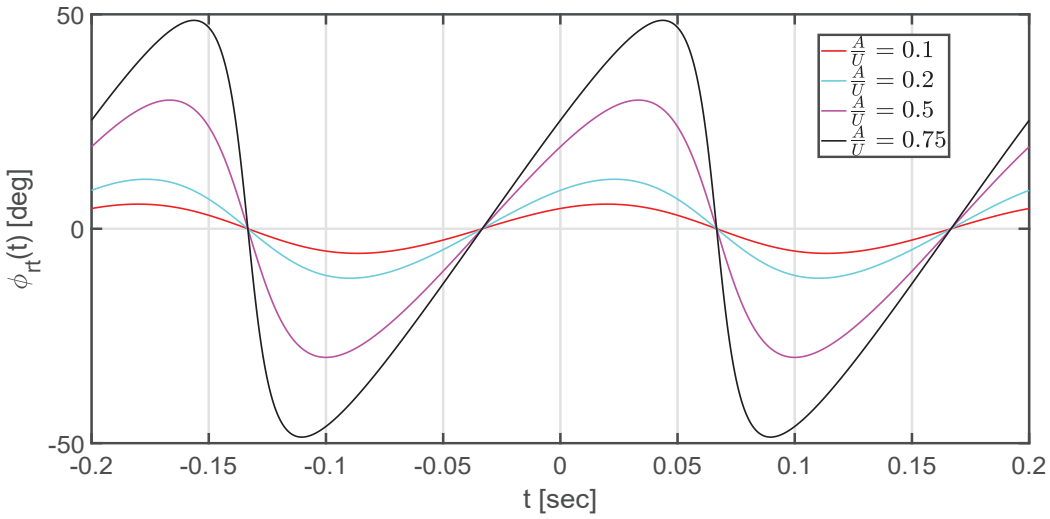

Figure 1.13.: ϕ_{rt} versus t for $f_a = 35Hz, f_u = 30Hz$ and $\frac{A}{U} = 0.1, 0.2, 0.5, 0.75$ with $U = 1$ and $\alpha = \frac{\pi}{3}$.

Thus the value of the variable leading to the maxima (extrema) is reduced by the actual phase difference α and then stretched or compressed by the inverse of the difference of the angular velocities. The distance from the beginning of one periode, zero-crossing with $\dot{\phi}_{rt} > 0$, to t_{max} follows by (1.53) with $\alpha = 0$:

$$t_{max} = \frac{1}{\Delta\omega} \arccos[-\frac{A}{U}]. \tag{1.53}$$

The point symmetry of the $\arctan$ to the half of its period length $\frac{\Delta T}{2}$ allows to calculate the time from the beginning of the periode to the minima as:

$$t_{min} = \Delta T - t_{max} \tag{1.54}$$

$$= \Delta T - \frac{1}{\Delta\omega} \arccos[-\frac{A}{U}], \tag{1.55}$$

whilst the time between the maxima and minima equals:

$$\Delta t_{max,min} = t_{min} - t_{max} = \Delta T - \frac{1}{\Delta\omega} \arccos[-\frac{A}{U}] - \frac{1}{\Delta\omega} \arccos[-\frac{A}{U}] \tag{1.56}$$

$$= \Delta T - \frac{2}{\Delta\omega} \arccos[-\frac{A}{U}]. \tag{1.57}$$

In contrast to the scenario analyzed first, the vector $\vec{A}(t)$ added in the second oscillates with an angular velocity ω_a, which differs from ω_u. This difference of angular velocities causes the phase of the resulting vector $\vec{R}(t)$ with respect to the original vector $\vec{U}(t)$ and the absolute value of $\vec{R}(t)$ to depend on time t with a periodicity given by (1.49). Thus, the first constellation, not depending on time, is classified as static and the second one as dynamic. Once attained the relative relation between the vectors does not change in the static setup, all values possible for $\vec{R}_{rt}, \phi_{rt}$ for a given parameter set $U, A, \alpha, \Delta\omega$ are embraced within the time interval ΔT.

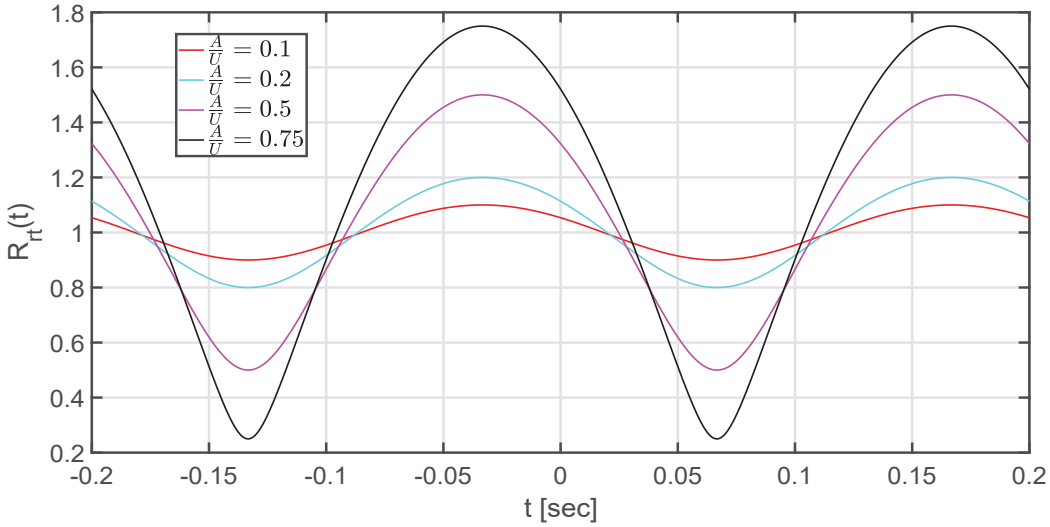

Figure 1.14.: Resulting vector length R_{rt} versus time t for $f_a = 35Hz, f_u = 30Hz$ and $\frac{A}{U} = 0.1, 0.2, 0.5, 0.75$ with $U = 1$ and $\alpha = \frac{\pi}{3}$. Note: The courses deviate from the ordinate value one in an unsymmetrical manner.

1.3. Technical Context

Regardless of its specific technical context any quantity represented by the oscillating vectors $\vec{U}(t), \vec{A}(t)$ has to be detected by a receiver and displayed before it can be interpreted. Hence, in order to interprete the gathered data correctly, the receiver settings have to be taken into account. Any receiver integrates a signal over a time interval in order to generate one data point as to say output, e.g. for a display. Assuming a correspondingly chosen averaging, neither the length nor the placement of the integration interval relative to the signal will alter the outcome in the static setup. In the dynamic case (1.45), (1.46), (1.47) describing the signal due to the superposition, its absolute value, its phase deviation, respectively change with the observation time. Based on these equations and, even more intuitively, based on the plotted course of the phase deviation, figure 1.13, and the resulting absolute value, figure 1.14, it becomes clear, that the length of the interval, as well as its start and end, can have an impact on the datapoint. For instance, due to the point symmetry to $n\frac{\Delta T}{2}$ with $n \in \mathbb{Z}$, the integral of the phase deviation yields zero, if the integration interval is equally spaced around $n\frac{\Delta T}{2}$. In contrast to that, the function describing the absolute value is not point symmetric to any point of its period ΔT. Thus, even integrating it over exactly one period ΔT will result in an offset with respect to the undisturbed oscillation.
Up to this point, the superposition of two vectors in the static as well as in the dynamic scenario has been treated solely mathematically. This gives rise to the reasonable question: What sparks the motivation to do so at all? There is a large variety of technical frameworks in which vectors describe the quantities involved and thus in turn not only offer a qualitative insight into their superposition, but also allow for quantifying the outcome of the latter.
Every acquisition of a signal is accompanied by noise, regardless whether it is of electrical or acoustical nature. Here, the vector $\vec{U}(t)$ resembles either the signal itself or one of its Fourier components whilst the additional $\vec{A}(t)$ describes a noise component. Based on this concept, additionally including measurement uncertainties Geise and Geise [8] for instance derive the required dynamic measuring range for a desired phase as well as magnitude uncertainty.
Another example for vector addition refers to antenna measurement; $\vec{U}(t)$ refers to a continuous wave signal at measurement frequencies and $\vec{A}(t)$ might be a component reflected at an absorbing wall. Whereas the amplitude is known directly due to the absorber properties, the phase of $\vec{A}(t)$ can be considered a random variable.

In addition to a cw scenario, the presented vectorial approach even allows to model the impact of multipath propagation on modulated signals and thus in turn upon transferring information e.g. in the realms of navigation; GPS [9, p. 257], ..., DME, (D)VOR. For instance, in case of the (D)VOR this can be the 30 Hz sideband modulation superimposed with an undesired 35 Hz signal, which may come from a non-static scatterer.
The very high frequency omnidirectional radio range (VOR) and its follow up version, the Doppler VOR (DVOR), whose functionality is explained in more detail at the beginning of chapter 2, has become a very timely topic. The (D)VOR is a navigation system, the ground station of which provides bearing intelligence over a radius of up to 300 km [81]. One of two signals delivers the actual bearing intelligence by its relative phase, whilst the second signal — emitted in an omnidirectional manner — serves as reference.
Aside from the finite nature of fossil energy sources, their contribution to the climate change due to using them and consequently other related effects of global impact have generated the public motivation to reduce the dependency on them. Alternatively, using energy created by nuclear fission has created the longterm problem of having to store its waste. The accident 1986 in Tschernobyl and ultimately the disaster 2011 in Fukushima have sparked a big momentum in the green energy movement. This is reflected e.g. by the fact, that the German Bundestag in 2011 decided to abandon nuclear energy completely, the Renewable Energy Law, in German *Erneuerbare Energien Gesetz* (EEG), and the considerations regarding a climate neutral Germany [10].
Despite the knowledge of these in terms of humanity self-created existential problems it is most likely that the demand for energy keeps increasing. Paired with the common lethargy with respect to act upon the obvious problems at hand, this demand urges to assess renewable sources. Amongst these wind energy constitutes a major portion [11]. Of course areas with a high wind intensity most likely offer the best chances for wind turbines. A higher hub height and longer rotor blades increase the efficiency of a wind turbine. This is why nowadays wind turbines have their hubs 120 m or higher above the ground whilst their blade length can reach 65 m and more. For such or constructions lightning protection is mandatory, so a metal structure of some kind is incorporated. This in turn increases the potential interaction of a wind turbine with electromagnetic waves. The touching point between the wind energy and the (D)VOR is that many ground stations were built in windy areas. In order to protect the bearing intelligence from impairing effects, the International Civil Aviation Organization (ICAO) has defined building restricted areas (bra). Figure 1.15 schematically depicts the cross-section of the bra the center of which corresponds to the center of the antenna array on the ground. The bra consists of one cone with an elevation angle of 1° and two concentric cylinders. In case of a conventional VOR the bigger radius equals 15 km, in case of a Doppler VOR 10 km. Thus, to be more precise the bra defines a volume. And as soon as any intended construction enters this volume the ICAO requires to individually investigate its impact upon the signal in question. In addition to that the ICAO recommands to always investigate the influence of tall constructions; skyscrapers, TV-towers and such alike [12].
In Germany the §18a LuftVG regulates that the federal offic of flight saftey, in German Bundesamt für Flugsicherheit (BAF), is to decide, whether an intended construction can have an impact on services related to flight safety. This decision is to be based on a consultant's advisory opinion. Here the BAF relies up to now exclusively on the Deutsche Flugsicherung (DFS). According to a poll [13] conducted by the German Wind Energy Association, in German *Bundesverband WindEnergie (BWE)*, in 2015 a wind power equivalent of 2333 MW could not be realized due to the DFS's ostensible safety concerns regarding VHF omnidirectional radio range, 39 of the total of 59 in the BRD are of the Doppler type. In 2019, the BWE repeats the survey with higher degree of detail [14]. This update reveals that currently planned and financially backuped wind turbines equivalent to 1680 MW are denied to be installed due to VOR and 3109 MW due to DVOR safety concerns. By considering a financial investment of

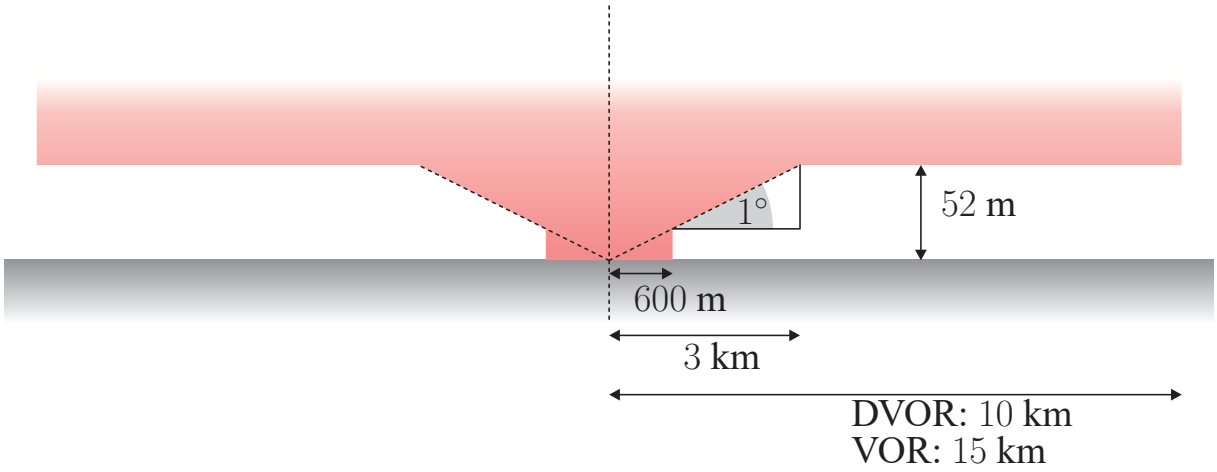

Figure 1.15.: Cross section of the axially symmetrical building restricted area (volume) according ICAO EUR DOC 015.

1.5 million Euro per MW this corresponds to about 2.5 billion Euro and 4.7 billion Euro on hold due to the DFS's assessment of concerns regarding the VOR and DVOR, respectively. Of course safety concerns have to be taken seriously. A manifold of reasons such as

- the fact that no physical reasoning is given for the design of the bra,
- the fact that in 2017 Belgium has reduced the radius down to 7 km beyond which wind turbines footnotesizeer than 200 m in height get approved without having experienced drawbacks in flight navigation [15, 16],
- the flaws in the technical argumentation of the DFS [17],
- the increasing number of court procedures with the DFS on one and wind power operators on the other side,
- ...
- the fact that political issues seem to dominate the way how this conflict of interests is handled

prove the high demand of a solid understanding of the involved physics, the need to understand, which quantities do have an impact on the output of an ideal receiver and the need for the capability to quantify their impact on it.